SPE 111853

Meeting the Challenges of Real-Time Production Optimization—A Parametric Model-Based Approach

Ankur Awasthi, University of Houston; Sathish Sankaran, SPE, Halliburton-Landmark; Michael Nikolau, SPE, University of Houston; and Luigi Saputelli, SPE, and Gerardo Mijares, SPE, Halliburton-Landmark

This paper was prepared for presentation at the 2008 SPE Intelligent Energy Conference and Exhibition held in Amsterdam, The Netherlands, 25–27 February 2008.

Abstract

The challenges to achieve real-time production optimization (RTPO) of oil and gas fields lie in the integration of asset-wide operations at multiple time scales, knowledge of reservoir phenomena, and efficient data management. Traditional approaches to production optimization workflows often make simplifying assumptions and work within artificial boundaries, to lower the complexity of an all-encompassing optimization problem. While this decomposition creates manageable workflows, it does not adequately support the integration of production optimization at multiple levels.

We propose a methodology to achieve hierarchical decomposition of the overall production optimization problem at different time scales, where real-time data are consistently used to identify reservoir performance and optimize production. The optimization tasks at each of these levels are organized through automated transactions of targets, constraints, and aggregate measurements. For example, strategic decisions such as long-term (e.g., yearly, monthly) injection targets, production plans etc. calculated using a full-physics reservoir model are resolved into tactical decisions for short-term (e.g., weekly, daily) production planning.

A moving-horizon based parametric model is proposed to provide fast predictions for production optimization in the short-term framework. Since the model structure is based on the decomposition of a full-physics reservoir model, it is reasonable to expect that the parametric model will be robust enough to be used for extrapolation outside the range of history data, a property needed for optimization purposes. In this paper, we present an analysis of the structure of the physics-compliant empirical model, the model's range of applicability, techniques that can be used for parameter identification, and use of the model for short-term production optimization. The paper presents a number of case studies to illustrate the benefits of the proposed methodology and its application in typical workflows for closed-loop reservoir management.

Introduction

The oil and gas industry is facing remarkable challenges to maximize profitability in a dynamic and uncertain environment while satisfying a variety of constraints. In response to such challenges, efforts have been made to improve oilfield operations by using better technology and appropriate business processes, among other things. A recent approach has been to adopt proven and successful technology from downstream (oil refining) and other related industries to solve related problems in upstream processes. While this approach is promising technologies and the processes have to be adapted to suit the needs of the oil and gas industry.

Current practices of production optimization often involve combining mathematical models, field data and experience to make decisions about optimal production scenarios. Often, mid-term decisions are made by performing multiple future production scenario forecasts and selecting the best scenario. However, the selected scenario may not be followed in practice due to various inevitable practical difficulties. As a result, it is required to feedback the deviations from the plan and dynamically reoptimize under the most current production conditions. But updating the numerical reservoir model with new field data through history matching is a laborious task exacerbated by the increasing number of real time measurements available today that increase the frequency at which field data can be collected. In addition, production optimization is limited by the discrepancy between the models used by reservoir and production engineers to address the holistic production optimization of the entire field at all time scales. With increasing emphasis on risk analysis that requires several runs of large numerical models, it is imperative to use alternative methods.

In recent literature, a number of proxy modeling techniques [1-10] have been proposed where the output variables (oil recovery factor, multiphase flow rates etc.) are modeled as a function of the input variables. However, most of these methods focus on data-driven approaches such as response surface techniques based on regression, interpolation, neural network etc. These methods are relatively easy to setup and capture the nonlinear effects in the training data set. However, reservoir phenomena unseen in the past (e.g., water breakthrough) or operating regimes that lie outside the range of training data set are not adequately predicted by such models. Further, most proxy modeling approaches used in production optimization actually model the reservoir simulator outputs and are seldom validated against real field data.

Brouwer et al [11] presented a vector-matrix representation of the reservoir model to employ optimal control and continuous model updating. The authors of this paper adopted this representation of the model to develop a parametric modeling methodology for Real-Time Production Optimization (RTPO) strategy [12, 13]. Since the parametric model structure is derived from reservoir physics, it is expected that the model will be suitable to extrapolate outside the training data set. A feasible approach to continuous model updating and short-term forecasting using this approach was presented in [14].

In this paper, we focus on the application of this modeling paradigm towards real-time production optimization of oil and gas fields. This provides the integrated model combining the reservoir and production engineering domains. The methodology used for production optimization is based on a multi-scale resolution of the problem – namely long-term, mid-term and short-term optimization. The long-term optimization is typically performed over the life of the field considering uncertainties and various field exploitation scenarios. The mid-term optimization focuses on maximizing the profitability following the optimal exploitation plan (in the order of weeks to months); whereas the short-term optimization computes the optimal daily production plan subject to constraints and targets passed down from the mid term optimization results.

In the rest of the paper, an overview of the multi-time scale RTPO approach is presented followed by a discussion of modeling issues related to real-time decision making. The formulation of the parametric model is presented thereafter followed by the methodology for continuous model updating using field data. The next section describes the formulation of the multi-time scale optimization problem and the results of the proposed approach on case studies.

Multivariable Optimization and Control in the Oil Industry. Historically, multivariate optimization combined with modeling techniques such as neural networks, genetic algorithm and fuzzy logic, etc., have been used in different ways in the oil industry to solve problems related to resource scheduling, reservoir history matching, production parameter settings [15], optimum well placement, and optimization of the recovery factor or displacement efficiency [11, 15, 16]. Such an optimization uses models generated either using basic first principles or data-driven models. With recent technological advancements, the industry has started to deploy downhole and surface measurement and control to measure key system parameters and to automate many of those tasks.

Figure 1 [12, 17-19], shows the different layers of the industrial automation hierarchy as applied to the oil industry. While the lower levels of the hierarchy compute the manipulated variables and feedback deviations from targets to the upper layers, the results of the upper layers act as corrective set-points to the lower ones, working as a closed-loop system. Several authors [15, 16, 20, 21] have proposed some optimum control theory strategies for enhancing oil recovery in steam, CO_2, gas and water injection projects. In most of these strategies, a control variable is manipulated while an objective function is optimized subject to a number of constraints. The implicit assumption in the above decomposition of the hierarchy into different time scales is that the aggregate of the individual optimum decisions at each level will be close to the overall optimal decision at each point in time. This assumption can be argued based on the fact that decisions made at a certain level pass corresponding targets downwards to the underlying level, which in turn attains such targets almost instantly with respect to the time-scale of the decision-making level. Even though the multi-level decomposition cannot guarantee a global optimum, it nevertheless makes an otherwise unsolvable problem feasible. In the next section, we outline the model reduction approach that allows consistent models to be used to make mid-term and short-term decisions.

Short-term Parametric Reservoir Model: Background

In practice, reservoir simulation is the *de facto* industry standard for reservoir management. However, the increasing industrial attention to RTPO requires tools capable of responding immediately based on real-time field information. The development of advanced reservoir simulation technology leads to large, complex reservoir models. Although larger complex models result in better long-term predictions and overall field management, they often require high computational time. Also, the reservoir model needs to be constantly updated through history matching (adjusting the model parameters to match production history). History matching is often a lengthy task and may sometimes take a year or so to complete. By such time, additional discrepancies arise between the data used to update the model and the actual production. It is for this reason that, often in practice, proxy models are used for short-term decisions that are necessary for optimization of daily production.

Model Formulation. Here, we build upon our previous work on building short-term parametric models [14]. The formulation of the structure of the parametric model is done starting from first principles - conservation of mass and constitutive equations (Darcy's law, compressibility equations and capillary pressure equations). After discretization with respect to the spatial coordinates, the parametric model can be represented in a vector-matrix form as follows:

$$\hat{\mathbf{B}}\frac{d\hat{\mathbf{p}}}{dt} = \hat{\mathbf{T}}_m\mathbf{p}(t) - \hat{\mathbf{T}}_h\mathbf{h} + \hat{\mathbf{q}}(t) \tag{1}$$

where, $$\hat{\mathbf{p}}_{i,j,k} = \begin{bmatrix} p_o \\ S_w \\ S_g \end{bmatrix}_{i,j,k} \tag{2}$$

containing values of block oil pressure, water saturation and gas saturation, sufficient to complete the reservoir description at all discretization points (grid blocks) indexed by $[i, j, k]$. The vector $\hat{\mathbf{q}}$ defined as:

$$\hat{\mathbf{q}}_{i,j,k} = \begin{bmatrix} q_o \\ q_w \\ q_g \end{bmatrix}_{i,j,k} \tag{3}$$

contains all external fluid flows. The convention is that these external fluid flows are negative at production points, positive at injection points and zero at all other points. The matrices $\hat{\mathbf{B}}$ and $\hat{\mathbf{T}}_m$ are associated with formation volume factors and mobilities, while the matrix $\hat{\mathbf{T}}_h$ contains terms due to gravity forces and are functions of time.

As discussed in [14], for short-periods of time, the time-dependence of the matrices $\hat{\mathbf{B}}$, $\hat{\mathbf{T}}_m$ and $\hat{\mathbf{T}}_h$ in Eq. (1) is relatively weak. Therefore, these matrices can be considered to be approximately constant. Using this simplifying assumption, one can formulate a simplified input-output model of the reservoir described in Eq. (1) in the standard state-space form [22-24] as follows:

$$\begin{aligned} \frac{d\mathbf{x}}{dt} &= \mathbf{A}\mathbf{x}(t) + \mathbf{B}\mathbf{u}(t) \\ \mathbf{y}(t) &= \mathbf{C}\mathbf{x}(t) + \mathbf{D}\mathbf{u}(t) \end{aligned} \tag{4}$$

where the vector $\mathbf{x}$ comprises the states of the system, namely the values of p_o, S_w and S_g at all discretization points in the reservoir (indexed by $[i, j, k]$ in Eq. (2) - (3)); the vector $\mathbf{y}$ captures the measured outputs (i.e., the production rates of oil, water and gas) in Eq. (3); the vector $\mathbf{u}$ captures the effect of inputs (i.e., bottomhole pressures (BHP's) and injection flow rates. The matrix $\mathbf{A}$ captures the internal dynamics of the reservoir; matrix $\mathbf{B}$ shows the effect of inputs on the states and matrix $\mathbf{C}$ generates measurable outputs from system states $\mathbf{x}$. While the streamlining of Eq. (4) from Eq. (1) has been extensively discussed [13, 14], we will briefly outline them here:

- Although Eq. (1) describes the time evolution of p_o, S_w and S_g at all grid blocks inside the reservoir, these values are not always measured (even at grid blocks associated with producers and injectors). But the external flow rates at the injector or producer grid blocks can be either measured using a multiphase meter or estimated through back allocation. While the output vector $\mathbf{y}$ contains values of $\hat{\mathbf{q}}$ at grid blocks with injectors and producers, it can be related to the state vector $\hat{\mathbf{p}}$ and the input $\mathbf{u}$ via equations of the form (Eq. (B.20) in [20])

$$\hat{\mathbf{q}} = \hat{\mathbf{W}}(\hat{\mathbf{p}}_{wf} - \hat{\mathbf{p}}) + \hat{\mathbf{w}}_{pc} \tag{5}$$

where, $\hat{\mathbf{p}}_{\mathbf{wf}}$ is the well bottomhole pressure (BHP); and $\hat{\mathbf{w}}_{pc}$ captures the capillary pressure effects. Substitution of $\hat{\mathbf{q}}$ from Eq. (5) into Eq. (1) results in a manipulated input $\mathbf{u}$ for the entire system which consists of the bottomhole pressures of producers or injectors.

- Although, the state vector $\hat{\mathbf{p}}$ of the system in Eq. (1) has physical significance, the natural order of the system dynamics is very high corresponding to the number of grid blocks considered in the discretization of the reservoir. However, the input-output model behavior of the system i.e., the effect of bottomhole pressures and injection rates on the production rates at producer grid blocks is expected to be represented by a reduced-order model. Therefore, the state vector $\mathbf{x}$ in Eq. (4) does not need to have physical significance in the same way as $\hat{\mathbf{p}}$ but will assist in capturing the input-output behavior of the reservoir.

- As mentioned, the matrices $\mathbf{A}$, $\mathbf{B}$, $\mathbf{C}$, $\mathbf{D}$ can be considered approximately constant for short-term predictions i.e., days to weeks. However, they will require an evaluation scheme to maintain the accuracy of the estimated model for short-term prediction purposes as new measurements are available from the field.

- The model matrices $\mathbf{A}$, $\mathbf{B}$, $\mathbf{C}$, $\mathbf{D}$ are estimated from the available measurements and reported field outputs over a period of time reported in the past using system identification concepts, while continuously updating the model to maintain the accuracy for short-term predictions. Because there are multiple inputs and outputs involved in any reservoir, subspace identification method [25-27] is used because of its relative simplicity, generality, numerical robustness and particularly suited for multivariable models.

The model parameters of the identified model are updated continuously when the field data is available (e.g., daily) using a moving horizon approach. The updating procedure maintains the accuracy of the model while retaining its inherent structure and will be discussed in detail in the next section.

Continuous Model Updating: Moving Horizon Approach. Both in the identification of the parametric model and its use by the optimization algorithm, it is required to reduce the uncertainty of the data used and the effect of decisions on outcomes. For example, if there were complete information about the behavior of the system into the future, one would not need to perform an optimization continuously. However, uncertainty is always present in future predictions, thus making feedback based continual decision making necessary. In addition, what is currently uncertain will be less uncertain in the future as new measurements are made and additional data become available. Nikolaou et. al [12] discusses the effect of uncertainty on the dynamic programming formulation of the optimization problem, which requires evaluating the objective function at distinct values of the state vector $\mathbf{x}_i(t+dt)$ with *t* going to infinity. This uncertainty creates a huge number of paths to consider for optimization from time t. To avoid this so-called "*curse of dimensionality,*" heuristic alternatives such as the concept of *moving horizon* or *receding horizon* are particularly useful.

The following steps outline the method to develop such short-term parametric models, refine them using the moving horizon approach and apply them to different production operation workflows.

- Data Acquisition: Select the model inputs and outputs relevant to the workflow using the available field measurements at the injectors and producers. The bottomhole pressures of the producers, and the injection rates as the manipulated inputs $\mathbf{u}$, and the multiphase rates at the producers as the measured outputs $\mathbf{y}$ are appropriate choices for production forecasting and production optimization related workflows. Figure 2 illustrates typical inputs and outputs for the parametric reservoir model.
- Data Validation: Pre-process field data for the selected inputs and outputs by removing outliers, non-zero means and non-stationary trends.
- System Identification: Select system identification parameters such as identification horizon, model order, and identify the model with the production data using the moving horizon framework on a periodic (e.g., daily) basis.

The parametric modeling methodology discussed above has been applied to the production forecasting workflow [14]. Future predictions were made based on a production and injection plan, assuming all inputs were known (even in the future) based on the initial plan. The reasonably accurate short-term (days) and mid-term (weeks) predictions for the different case studies showed that the reservoir behavior can be captured with the proposed approach. In the following section, we will discuss how such a parametric model can be used within a production optimization framework.

Simultaneous Control and Optimization

In the context of the hierarchy presented in Figure 1, we will focus on demonstrating how we can use the aforementioned parametric model approach in making optimal decisions at different time scales (from days to weeks) corresponding to different levels of the hierarchy. The decisions passed down from the higher levels (e.g., monthly production and injection rate targets calculated on an annual basis) must be consistently resolved into daily targets, knowing the short-term production schedule and field constraints. Current work processes and commercial applications often make simplifying assumptions and do not support such integration of production optimization at multiple time scales. Figure 3 shows the structure resulting from the interconnection of the various levels similar to the self-learning reservoir management methodology proposed by Saputelli et al [28]. The short-term parametric model is used to make forecasts which feed the net present value (NPV) block in the upper level. Optimization of the NPV objective function produces multiphase rates as set-points that are then fed to the underlying layer, working in a closed-loop.

Mid-Term Optimization – Maximizing NPV. The upper optimization level optimizes an NPV objective function using the current parametric reservoir model and subject to bottomhole and surface constraints. Net present value calculations are based on the following economic model [28]:

$$NPV = \max \sum_{k=1}^{N} \frac{[(q_o^k R_o + q_g^k R_g - q_w^k C_w - q_{w,inj}^k C_{w,inj})\Delta T_k]}{(1+d)^{\frac{k\Delta T_k}{365}}} \tag{6}$$

where, q_o^k, q_w^k and q_g^k are the daily production rates of oil (STB/d), water (STB/d) and gas (SCF/d), at time interval k; $q_{w,inj}^k$ is the daily injection rate of water (STB/d); R_o and R_g are the net selling prices of oil ($/STB) and gas ($/SCF); C_w and $C_{w,inj}$ are the cost of treatment of produced and injected water respectively; d is the annual discount factor and N is the number of time intervals or the prediction horizon.

The above equation is subject to the following downhole and surface constraints on the bottomhole pressure (p_{wf}) and the tubing head pressure (p_{tf}) respectively:

$$p_{wf,\min} \le p_{wf} \le p_{wf,\max} \tag{7}$$

$$p_{tf,\min} \le p_{tf} \le p_{tf,\max} \tag{8}$$

The above optimization exercise is carried on with the information available at each time step assuming the reservoir can be described by the parametric model derived in Eq. (4). As time progresses the model is updated, and the NPV will be refined continuously. However, due to the linear nature of the parametric state-space model, Eq. (6) results in a linear objective function and is solved using a linear-optimization routine to find the optimum solution.
Eq. (6) can be further simplified in a compact linear form (see Appendix A) as follows:

$$\begin{aligned} &\max_u \{\mathbf{f}_1^T \mathbf{u} + \mathbf{f}_2\} \\ &\mathbf{A}_l \mathbf{u} \le \mathbf{b}_l \end{aligned} \tag{9}$$

Short-Term Optimization. The set-points once passed from the upper layer in the hierarchy are used by the underlying layer for feedback control. Consistent with the decision making hierarchy described earlier, the parametric model can be used for such short-term optimization or control purposes. Thus, the production optimization problem can be stated as:

"Given the operational availability and targets for all wells, calculate the optimum daily production plan or the well flowing pressures (thus, production rates) and injection rates, subject to field constraints."

We use a model predictive control (MPC) strategy [29-31], a class of control algorithms that explicitly uses a process model for predicting plant behavior and computing the optimum control action through online optimization of an objective function over a horizon, subject to constraints. The development of MPC is based on the block diagram shown in Figure 4.

The main steps here are to measure the plant output $\mathbf{y}(t)$, estimate the states $\hat{\mathbf{x}}(t)$, and deliver a control action to the plant input $\mathbf{u}(t)$ while trying to track the set-points and rejecting plant disturbances. The goal of the state estimator is to determine the optimal approximation to the state evolution based on current and past inputs and measurements.

The optimization problem is set up using the standard MPC formulation with the objective function as follows:

$$\min_{\mathbf{u}^M}\Big[\sum_{j=1}^{P}(\mathbf{y}_{k+j}-\mathbf{y}^{sp}_{k+j})^T\mathbf{W}_{\mathbf{y}}(\mathbf{y}_{k+j}-\mathbf{y}^{sp}_{k+j})+\sum_{j=0}^{M-1}\Delta\mathbf{u}^T_{k+j}\mathbf{W}_{\Delta\mathbf{u}}\Delta\mathbf{u}_{k+j}\Big] \tag{10}$$

where P is the prediction horizon, M is the control horizon and $\mathbf{y}^{sp}_{k+j}$ is the vector of daily output targets received from the upper economic optimization layer, and $\mathbf{u}_{k+j}$ and $\mathbf{y}_{k+j}$ are the j-step-ahead vectors of manipulated inputs (e.g., well flowing pressure, injection rates) and measured outputs (e.g., production rates), $\mathbf{W}_{\mathbf{y}}$ and $\mathbf{W}_{\Delta\mathbf{u}}$ are the weighting matrices on output and input deviations respectively. The field (or the plant) is modeled using the parametric model described in Eq. (4), shown in discrete time, as follows:

$$\begin{aligned}\mathbf{x}_{k+j}&=\mathbf{A}\mathbf{x}_{k+j-1}+\mathbf{B}\mathbf{u}_{k+j-1}\\ \mathbf{y}_{k+j}&=\mathbf{C}\mathbf{x}_{k+j}+\mathbf{D}\mathbf{u}_{k+j}\end{aligned} \tag{11}$$

A Kalman filter is used to estimate the model states is given by:

$$\hat{\mathbf{x}}(k+1)=\mathbf{A}\hat{\mathbf{x}}(k)+\mathbf{B}\mathbf{u}(k)+\mathbf{K}(\mathbf{y}(k)-\mathbf{C}\hat{\mathbf{x}}(k)) \tag{12}$$

where, $\mathbf{K}$ is the Kalman gain estimated as part of the identification algorithm assuming a Gaussian measurement noise.

The above objective function is subject to the field constraints as follows:

$$\begin{aligned}u_{\min}&\le u_{k+j}\le u_{\max}\\ y_{\min}&\le y_{k+j}\le y_{\max}\end{aligned} \tag{13}$$

and

$$\Delta\mathbf{u}_{k+j}=\mathbf{u}_{k+j}-\mathbf{u}_{k+j-1} \tag{14}$$

Eq. (10) - (14) can be combined to give the following quadratic programming problem (see Appendix B):

$$\min_{\mathbf{u}}\{\mathbf{u}^T\mathbf{H}\mathbf{u}+\mathbf{u}^T\mathbf{f}\} \tag{15}$$

$$\mathbf{A}_c\mathbf{u}\le\mathbf{b}_c \tag{16}$$

The above quadratic problem can be solved efficiently online.

Results

The following example illustrates the closed-loop strategy in context to the multi-scale optimization problem described above. The results are compared to conventional practices of no control or reactive control i.e., reactive shut-in of zones with high water-cut. Figure 5 shows a two-layered reservoir with a line drive injector/producer also referred as the one-quarter 5-spot configuration. The reservoir has an upper, low-permeability layer and a lower high-permeability layer separated by an impermeable layer. A smart well completion is considered where remotely activated valves are available at each permeable layer so that both injection and production can be remotely adjusted. Both wells (injector and producer) are perforated at each of the two layers. The main production challenge for this reservoir is caused by the difference in permeability values (e.g., ratio 1:10) between the two layers.

The following production strategies are compared over a period of eight (8) years (summarized in Table 1):

- No control: Water is injected at a constant flow rate target in each layer.

- Reactive control: Water is injected at a constant flow rate target in each layer as in the no control case, but each perforated layer that exceeds a water-cut threshold value is shut-in.

- Closed-loop control: The decision variables are the bottomhole pressures of the two production layers and the flow rates of the two injection layers, while available measurements are the zonal multiphase rates. Thus for the given reservoir configuration in Figure 5, there are four variables to be manipulated. In the upper optimization layer, the parametric model is built based on the last 30 days of history to predict the multiphase rates by maximizing the NPV over a prediction horizon of next 30 days, subject to bottomhole and injection rate constraints for each production and injection layer respectively. As described in Figure 3, the optimum multiphase rates for the next four weeks are then passed on to the lower level where the inputs are manipulated to attain the set-points on a daily basis for the next 30 days (moving horizon). In the process, the 4x4 multivariable input-output model is updated daily, to account for any uncertainties and external disturbances.

Figure 6 (a) shows the cumulative oil and water production profiles for the field described in Figure 5. The proposed closed-loop control strategy results in a significant increase in the oil production while the production layer is shut-in for the reactive control as the water-cut increases above 70%. A significant increase in oil production results in a higher NPV over the entire production period. It is also noticeable that water breakthrough is delayed for the closed-loop control case by 210 days (average).

In Figure 6 (b), the cumulative injection rate (optimal) from the closed-loop control case is compared for both permeability layers. As water breaks through from the high-permeability layer, it is detected and controlled while maximizing the NPV. As more water is produced and water breaks through both layers (720 days), the model expects more oil to be produced from the high permeability layer than the low permeability layer thus injecting water in both layers but in a controlled manner.

The model parameters used for the closed-loop control case for the both the upper-level linear optimization and the lower-level quadratic optimization are shown in Table 2. The lower-level, quadratic optimization was performed by predicting a week ahead (P) while manipulating inputs only five days in the future (M). However, implementing only the inputs after the first day and then moving forward in time.

Figure 7 shows the optimum bottomhole pressure (BHP) profile for both layers compared to their respective average grid block pressure (PAVG). It should also be noted that the bottomhole pressures are constantly adjusted (daily), without any prior knowledge of the reservoir characterisitcs or the average reservoir pressure. As expected, the drawdown (differential pressure driving fluids from the reservoir to the wellbore) in the low permeability layer is higher compared to that for the high permeability layer to produce the same target oil rate.

Figure 8 shows the aerial view of the oil saturation distribution for the low permeability layer after 3000 days (end of simulation). For both the reactive control and the closed-loop control case, the fluid distributions are fairly similar except that the closed-loop control shows better vertical sweep efficiency. However, the high permeability layer as shown in Figure 9 shows more uniform oil saturation distribution using closed-loop control resulting in better vertical sweep efficiency.

A summary of the production strategies employed over a period of 8 years along with the NPV values and the oil recovery values are shown in Table 2. In the no-control and reactive-control cases, water injection is not guided by any economic objective. Rather, both injection layers are open and react to the reservoir pressure decline, driven by production. As a comparative result, the closed-loop control case was able to reduce cumulative water production (CWP) by 54% and reduce cumulative water injection (CWI) by 41% compared to the uncontrolled case, resulting in a NPV increase of $19 million. However, a comparison with the reactive control case shows an increase in the cumulative oil production (COP) by 0.9 MMSTB for original oil in place (OOIP) of 6.8 MMSTB resulting in a NPV increase of almost $12 million.

Model prediction

In previous sections, we discussed the importance of developing model structures as shown in Eq. (4) that do not violate first principles yet have parameters that can be identified in real-time from field data. While such a parametric model may not be perfect, it should al teast capture the elements of the reservoir dynamic behavior that are important for continuous optimization using feedback. The results of the model prediction of the closed-loop control case are shown in Figure 10 (a) and (b) for the low-permeability and high-permeability layer respectively. It can be seen that almost perfect agreement is observed between the parametric model and the field measurement, for both the cumulative oil and water production. However, it should be noted that a small deviation is observed between the predicted and the measured oil production, after water breaks through in the high permeability layer around 650 days. This error can be attributed to the fact that, although the model cannot predict the onset of water before water has broken through, it progressively adapts to the new conditions keeping this mismatch within reasonable limits.

Figure 11 shows the maximum eigenvalue of the daily updated parametric model. The estimated, maximum eigenvalue at each time step is very close to unity, which illustrates the integrating effect of the reservoir model. This result was also confirmed by the detailed eigenvalues analysis shown in [14], which outlines the following two scenarios:

- The matrix $\mathbf{A}$, has atleast 2 (and 3 for three-phase flow) eigenvalues exactly equal to zero irrespective of how the reservoir is discretized.
- For the special case of zero capillary pressure or zero capillary pressure gradients with respect to the water saturation, the matrix $\mathbf{A}$ has at least m x n zero eigenvalues (2-D reservoir discretization, (m, n)).

Conclusions

We have established a methodology to develop and continuously update short-term parametric models consistent with the full-physics reservoir model using well known methods of system identification for multivariable dynamical systems. These models can effectively provide short-term predictions (days to weeks) for the purpose of optimizing production in a multi-scale framework using a moving horizon formulation. The multi-scale architecture has two levels. The upper level that optimizes the NPV function (weeks) subject to physical constraints by calculating the optimum values of the production and injection flow settings. The upper level then passes these optimal values as set-points to the lower level, which uses a model-based predictive (MPC) control strategy to achieve these set-points on a daily basis.

An example demonstrated the possibility of using such a real-time closed-loop control strategy when applied to production or reservoir management projects, as compared with reacting to well performance. Further, the methodology considers the typical field production operations work processes to suit the data needs for the proposed approach. The strategy presented here can be refined in a number of ways, such as by fine-tuning various parameters, i.e., horizon lengths and weighting on the optimum values; analyzing the model to understand the phenomena of water breakthough and whether the model can be refined to predict it.

Acknowledgements

The authors acknowledge Halliburton and University of Houston for permission to publish this work. The authors acknowledge the following software contributions: VIP reservoir simulator from Halliburton and MATLAB.

Nomenclature

Boldface uppercase: Matrix
Boldface lowercase: Vector

q : Flow rate
S : Saturation
β : Terms with formation volume factor
N : Prediction horizon, NPV optimization
M : Model horizon, MPC
P : Prediction horizon, MPC
p_{wf} : Bottomhole flowing pressure
p_{tf} : Tubinghead pressure
R_o : Net selling revenues of oil, US, $/STB
R_g : Net selling revenues of gas, US, $/STB
C_w **:** Water operating expense, US, $/STB

$C_{w,inj}$: Water injection expense, US, \$/STB

d : Discount rate (%)

$\mathbf{u}$: Input vector

$\mathbf{y}$: Output vector

$\mathbf{x}$: State vector

$\hat{\mathbf{x}}$: Estimated state

$\mathbf{u}_{\min}$: Minimum value of input vector ay any given time

$\mathbf{u}_{\max}$: Maximum value of input vector ay any given time

$\mathbf{A}$: Matrix determining system dynamics

$\mathbf{B}$: Matrix determining input effects

$\mathbf{C}$: Matrix determining system outputs

$\mathbf{K}$: Kalman filter

$\mathbf{W}_y$: Penalizing the error between the output and the set-point

$\mathbf{W}_{\Delta u}$: Penalizing changes in inputs

$\hat{\mathbf{T}}_m$: Transmissibility matrix

$\hat{\mathbf{T}}_h$: Transmissibility matrix for gravity driven flow

$\hat{\mathbf{B}}$: Storage matrix

$\hat{\mathbf{A}}$: System matrix

Abbreviations
BHP: Bottomhole pressure
NPV: Net present value
MPC: Model Predictive Control
COP: Cumulative oil production
CWP: Cumulative water production
CWI: Cumulative water injection

Subscripts
o : Oil
w: Water
g: Gas
inj: Injection
k: Current time
m: Mobility term
h: Gravity term

Superscript
k: Predicted
sp: set-point (targets)

References

1. Chu, C., "Prediction of Steamflood Performance in Heavy-Oil Reservoirs Using Correlations Developed by Factorial Design Method". SPE Paper No. 20020. Presented at the *SPE California Regional Meeting*, Ventura, CA, 1990
2. Corre, P., P. Thore, V. de Feraudy, and G. Vincent, "Integrated Uncertainty Assessment For Project Evaluation and Risk Analysis". SPE Paper No. 65205. Presented at the *European Petroleum Conference*, Paris, France, 2000
3. Damsleth, E., A. Hage, and R. Volden, *Maximum Information at Minimum Cost: A North Sea Field Development Study With an Experimental Design.* Journal of Petroleum Technology, 1992. **44**: p. 1350-1356.
4. Dejean, J.P. and G. Blanc, "Managing Uncertainties on Productions Using Integrated Statistical Methods". SPE Paper No. 56696. Presented at the *Annual Technical Conference and Exhibition*, Houston, TX, USA, 1999
5. Egeland, T.e.a., "Designing Better Decisions". SPE Paper No. 24275. Presented at the *European Petroleum Computer Conference*, Stavanger, 1992
6. Eide, A.L., L. Holden, E. Reiso, and S.I. Aanaonsen, "Automatic History Matching by Use of Response Surfaces and

Experimental Design". Presented at the *4th European Conference on the Mathematics of Oil Recovery*, Røros, Norway, 1994

7. Friedmann, F., A. Chawathé, and D.K. Larue, *Assessing Uncertainty in Channelized Reservoir Using Experimental Designs.* SPE Reservoir Evaluation & Engineering, 2003. **6**: p. 264-274.
8. Güyagüler, B. and R.N. Horne, "Uncertainty Assessment of Well-Placement Optimization". SPE Paper No. 71625. Presented at the *Annual Technical Conference and Exhibition*, New Orleans, Louisiana, 2001
9. Landa, J.L. and B. Güyagüler, "A Methodology for History Matching and the Assessment of Uncertainties Associated with Flow Prediction". SPE Paper No. 84465. Presented at the *Annual Technical Conference and Exhibition*, Denver, Colorado, 2003
10. Manceau, E., M. Mezghani, Zabalza-Mezghani, and F. Roggero, "Combination of Experimental Design and Joint Modeling Methods for Quantifying the Risk Associated With Deterministic and Stochastic Uncertainties – An Integrated Test Study". SPE Paper No. 71620. Presented at the *Annual Technical Conference and Exhibition*, New Orleans, Louisiana, 2001
11. Brouwer, D.R. and J.D. Jansen, *Dynamic Optimization of Waterflooding With Smart Wells Using Optimal Control Theory.* SPE Journal, 2004. **9**(4): p. 391-402.
12. Nikolaou, M., A.S. Cullick, and L. Saputelli, *Production Optimization - A Moving Horizon Approach.* SPE 99358, 2006.
13. Nikolaou, M., A.S. Cullick, L. Saputelli, G. Mijares, and S. Sankaran, "A Consistent Approach toward Reservoir Simulation at Different Time Scales". SPE Paper No. 99451. Presented at the *Intelligent Energy Conference and Exhibition*, Amsterdam, Netherlands, 2006
14. Awasthi, A., S. Sankaran, M. Nikolaou, L. Saputelli, and G. Mijares, "Closing the Gap between Reservoir Simulation and Production Optimization". SPE Paper No. 107463. Presented at the *Digital Energy Conference and Exhibition*, Houston, TX, USA, 2007
15. Ramirez, W.F., *Application of Optimal Control Theory to Enhanced Oil Recovery*, ed. Elsevier. 1987.
16. Yeten, B., L. Durlofsky, and K. Aziz, *Optimization of Nonconventional Well Type, Location and Trajectory.* SPE Paper 77565, 2002.
17. Ng, K.M., *A multiscale-multifaceted approach to process synthesis and development.* ESCAPE, 2001. **41**.
18. Saputelli, L., M. Nikolaou, and M.J. Economides, *Self-Learning Reservoir Management.* SPE 84064, 2003.
19. Ydstie, B.E., *Distributed decision making in complex organizations: the adaptive enterprise.* Computers & Chemical Engineering, 2004. **29**(1).
20. Brouwer, D.R., *Dynamic water flood optimization with smart wells using optimal control theory*. PhD. Technische Universiteit Delft, 2004
21. Brouwer, D.R., G. Naevdal, J.D. Jansen, E.H. Vefring, and C.P.J.W. van Kruijsdijk, *Improved Reservoir Management Through Optimal Control and Continuous Model Updating.* SPE 90149, 2004.
22. Brogan, W.L., *Modern Control Theory*. 3rd ed, ed. P. Hall. 1991.
23. Chen, C.T., *Linear system theory and design*. 3rd ed, ed. O.U. Press. 1999.
24. Kailath, T., *Linear Systems*, ed. P.-. Hall. 1980.
25. Jolliffe, I.T., *Principal Component Analysis*. 1986: Springer-Verlag.
26. Ljung, L., *System Identification: Theory for the User*. 2nd ed. 1999: Prentice Hall.
27. Söderstrom, T. and P. Stoica, *System Identification*. Series in Systems and Control Engineering. 1989: Prentice Hall International.
28. Saputelli, L., *Self Learning Reservoir Management - An Application of Model Predictive Control for Continuous OIlfield Optimization*. PhD. University of Houston, 2003
29. Nikolaou, M., *Model Predictive Controllers: A Critical Synthesis of Theory and Industrial Needs*, in *Advances in Chemical Engineering Series*, G. Stephanopoulos, Editor. 2001, Academic Press.
30. Qin, S. and T. Badgwell, "An overview of industrial model predictive control technology". Presented at the *Fifth International Conference on Chemical Process Control - CPC V*. 1997.
31. Rawlings, J., *Tutorial overview of model predictive control.* IEEE Contr. Syst. Magazine, 2000. **20**(3): p. 38-52.

Figures

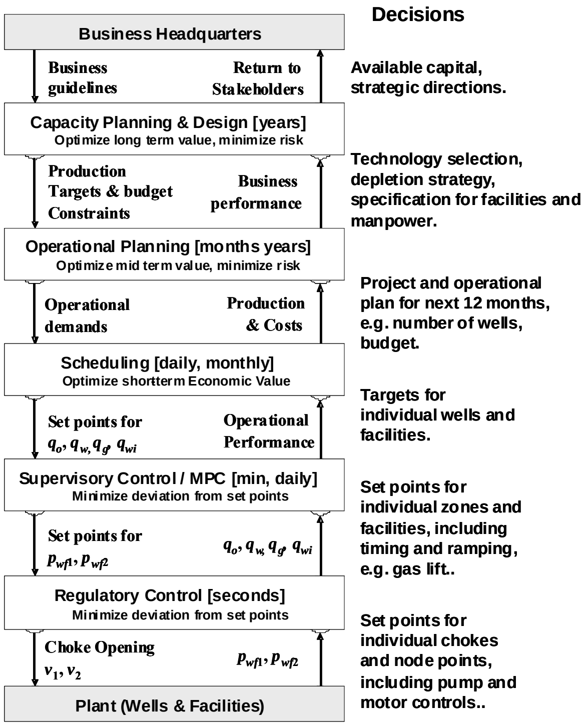

Figure 1: A multi-level hierarchy of oil-field decision making tasks at different time scales. Data movement is bi-directional and is passed from a lower level to an overlying level through the feedback loops while passing the decision as objectives and constraints to underlying level

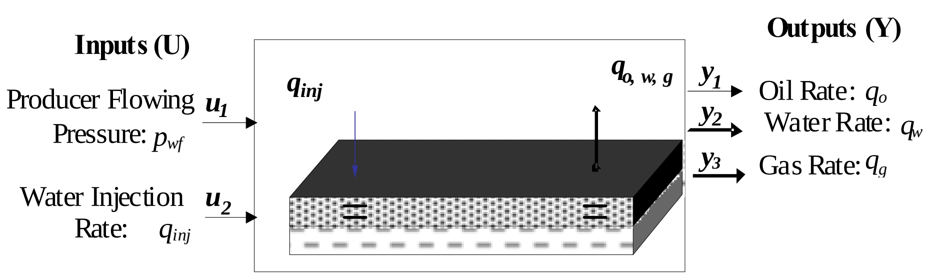

Figure 2: Injector producer example for a single layer reservoir showing all the inputs and outputs

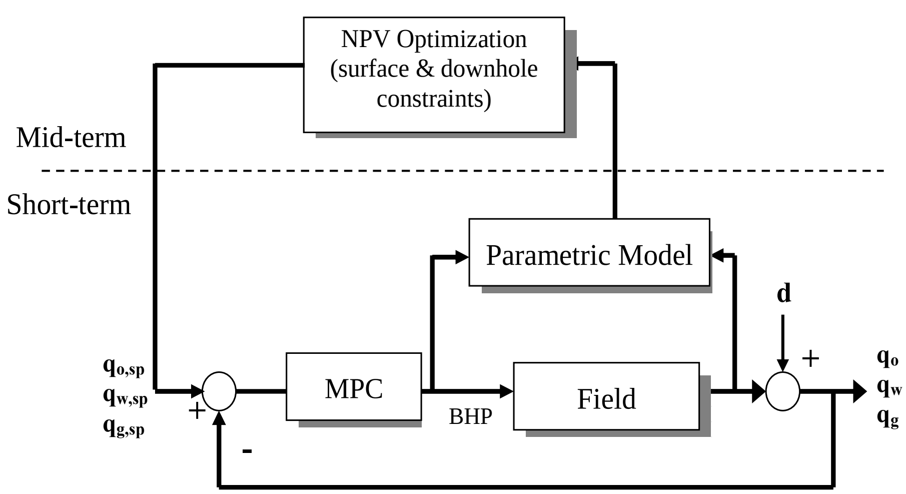

Figure 3: Multi-time scale production optimization framework

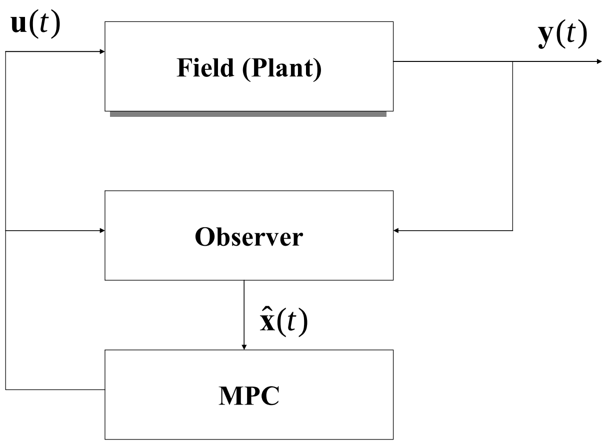

Figure 4: MPC block diagram

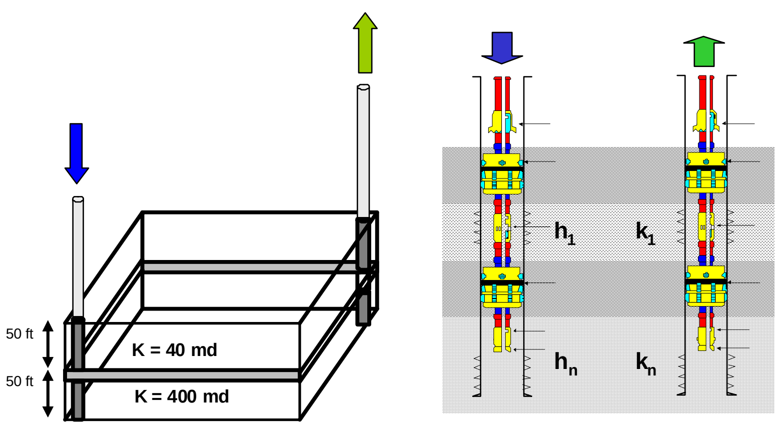

Figure 5: Reservoir and well configuration for a two layered reservoir, with one injector and one producer

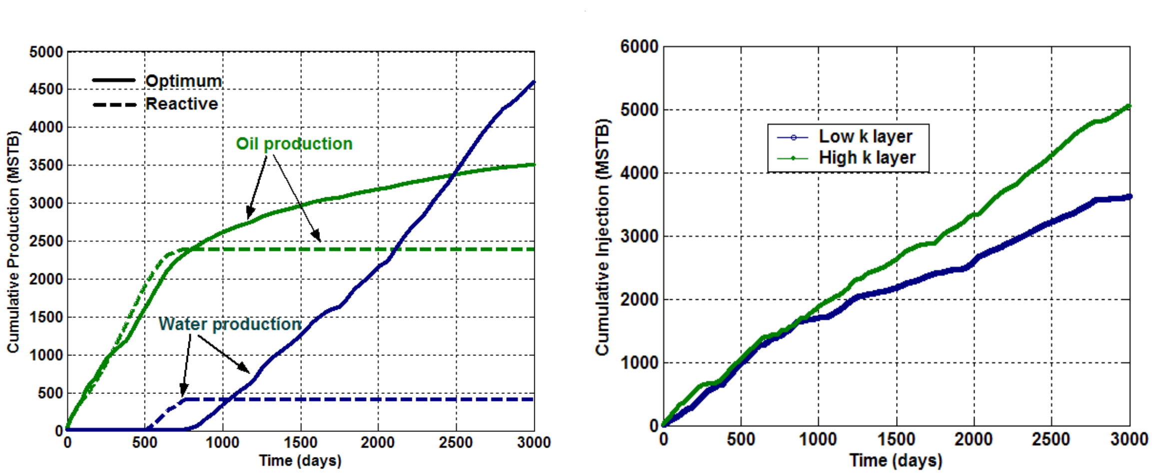

Figure 6: Cumulative production (MSTB) from the field (described in Figure 5) comparing reactive control and the closed-loop control (optimum) strategies (left plot). Cumulative injection (MSTB) profile in the closed-loop control case for both permeability layers (right plot)

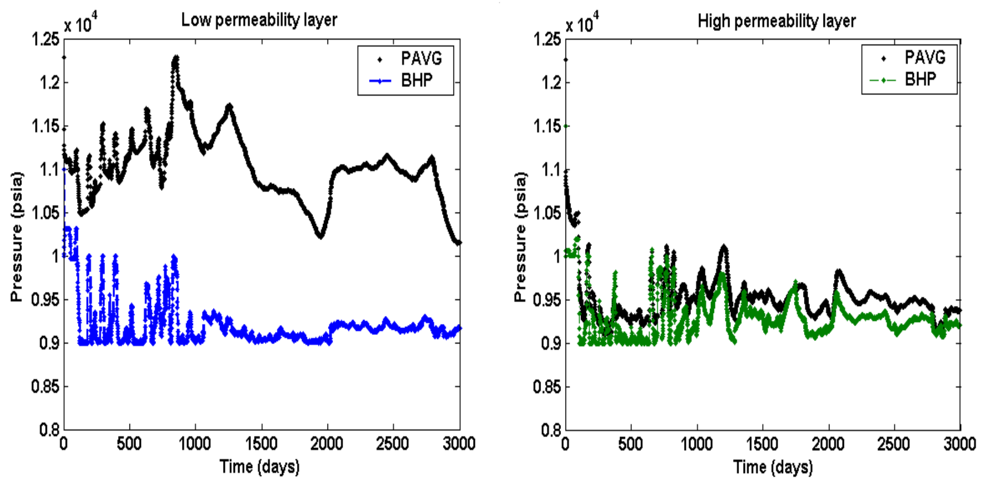

Figure 7: Daily manipulated bottomhole pressure for both permeability layers compared to the average block pressure

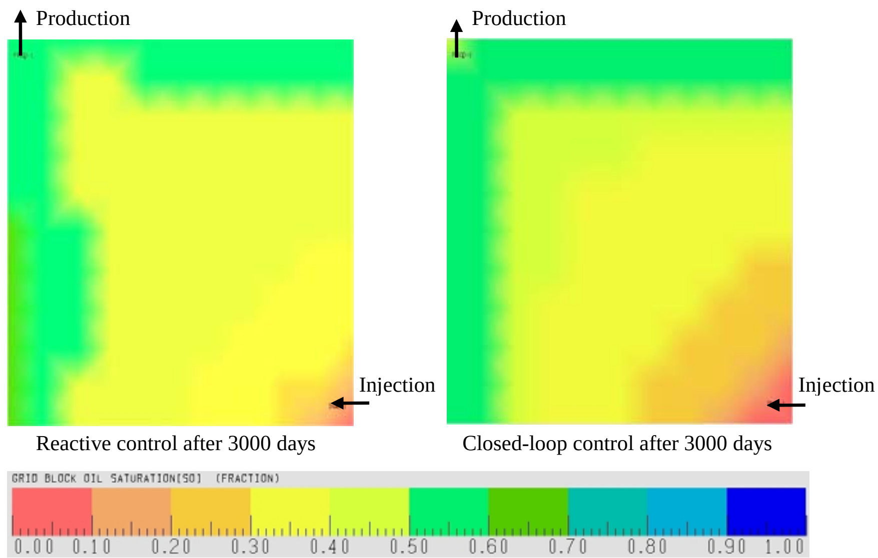

Figure 8: Oil saturation distribution (aerial view) of the low permeability layer for the two production scenarios i.e., reactive control and closed-loop control after 3000 days

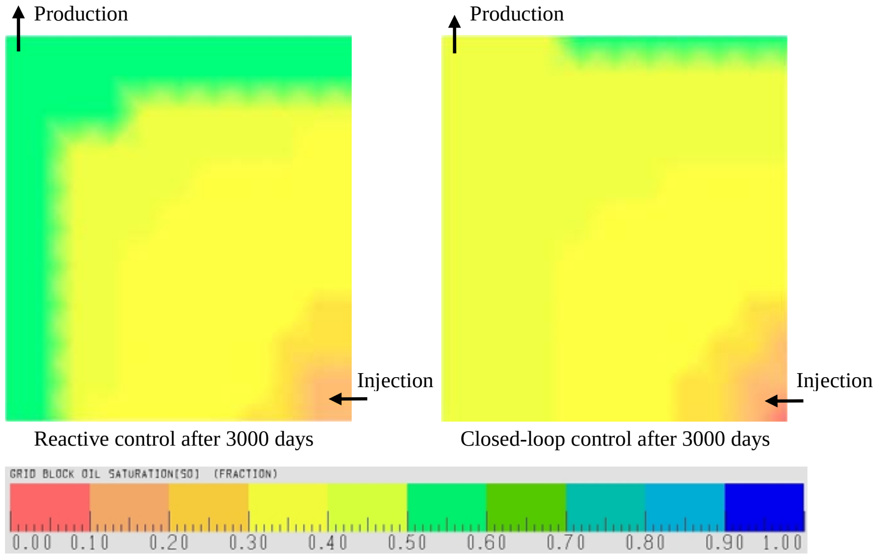

Figure 9: Oil saturation distribution (aerial view) of the high permeability layer for the two production scenarios i.e., reactive control and closed-loop control after 3000 days

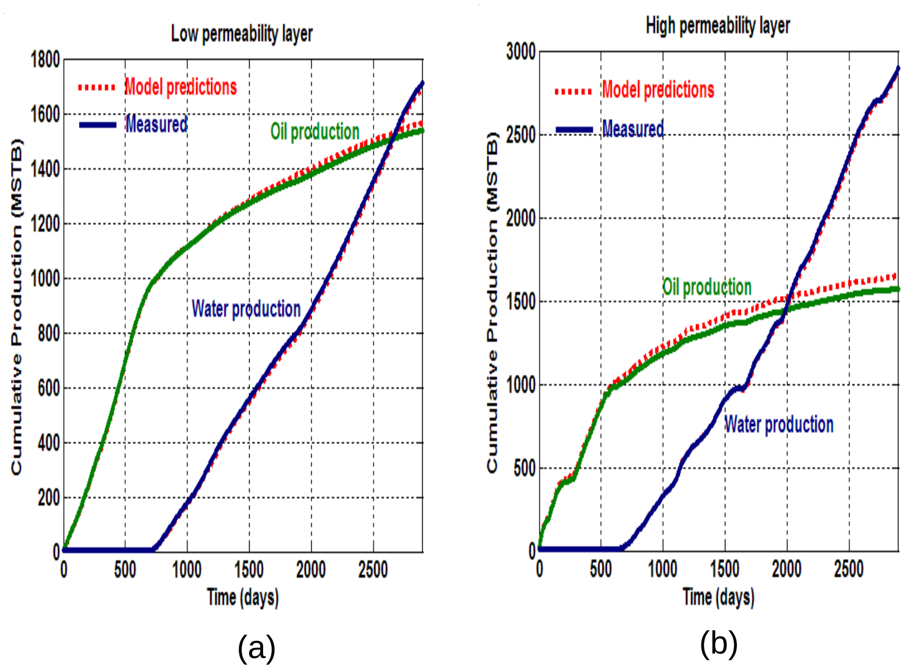

Figure 10: Cumulative oil and water production, comparison between the model prediction and the field measurement (optimum control case) for both the layers

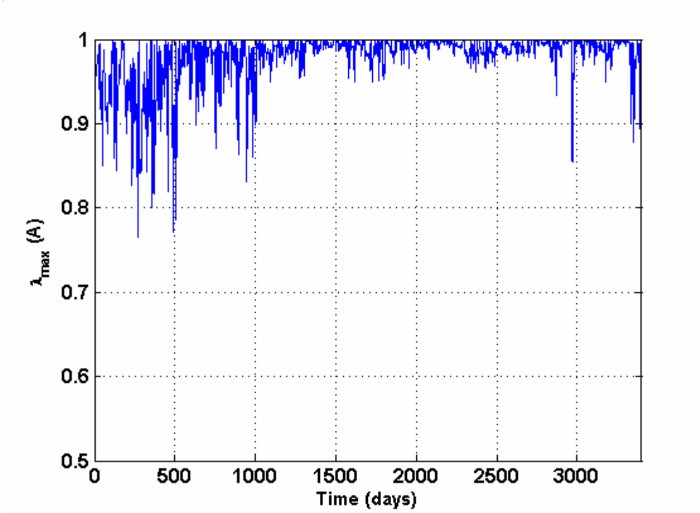

Figure 11: Maximum eigenvalues of matrix $\mathbf{A}$ in Eq. (4)

Tables

Table 1: Summary of production scenarios

Mode	Production scenario
No control	Constant injection target of 3000 STB (both layers)
Reactive control	Constant injection target of 3000 STB (both layers). Shut in production with WCUT > 0.7
Closed-loop control	Q_{max}<3000 STB BHP > 9000 psia (both layers)

Table 2: Model parameters (including economic data) used for closed-loop control

Variable	Value
$\mathbf{R_o}$: Oil price ($/STB)	30
$\mathbf{C_w}$, $\mathbf{C_{w,inj}}$: Average water-handling cost ($/STB)	2.5
d: Discount rate (%)	10
N: Prediction horizon (days) – NPV	30
M: Control horizon (days) – MPC	5
P: Prediction horizon (days) – MPC	7

Table 3: Summary of cumulative production rates, NPV and recovery

Production mode	NPV ($ MM)	COP (MSTB)	CWP (MSTB)	CWI (MSTB)	Recovery (%)
No control	47.7	3.6	10.1	14.7	52.9
Reactive control	54.6	2.4	0.4	5.1	35.3
Closed-loop control	66.3	3.5	4.6	8.7	51.4

Appendix A – NPV Objective Function Formulation

The objective function in Eq. (6), which is expressed as the finite sum of discounted cash flows during a horizon of N days:

$$NPV = \sum_{k=1}^{N} \frac{[(q_o^k R_o + q_g^k R_g - q_w^k C_w - q_{w,inj}^k C_{w,inj})\Delta T_k]}{(1+d)^{\frac{k\Delta T_k}{365}}} \tag{18}$$

where definitions are listed in the Nomenclature. The objective function is a simple one, with net selling revenues of oil and gas not taking into consideration the associated production costs.

To achieve an optimal solution of Eq. (18), a time model for q_o^k, q_g^k, q_w^k and $q_{w,inj}^k$ is assumed that evaluates the cash flow in time for given values of $R_o, R_g, C_w, C_{w,inj}, d$ and, finally, find a maximum value of Eq. (18) while satisfying system constraints.

Assuming the inputs and outputs for the two layered reservoir system in Figure 5:

$$\mathbf{u} = \begin{bmatrix} p_{wf1} \\ p_{wf2} \\ q_{inj1} \\ q_{inj2} \end{bmatrix} \text{ and } \mathbf{y} = \begin{bmatrix} q_{o1} \\ q_{o2} \\ q_{w1} \\ q_{w2} \end{bmatrix} \tag{19}$$

where subscripts 1 and 2 refer to variables in the low and high permeability layers respectively. The parametric model for the inputs and outputs in Eq. (19) over a horizon can be represented by the standard state-space form as follows:

$$\begin{aligned} \mathbf{x}_{k+j} &= \mathbf{A}\mathbf{x}_{k+j-1} + \mathbf{B}\mathbf{u}_{k+j-1} \\ \mathbf{y}_{k+j} &= \mathbf{C}\mathbf{x}_{k+j} + \mathbf{D}\mathbf{u}_{k+j} \end{aligned} \tag{20}$$

By combining the production costs (including the discount rate) associated with the outputs $\mathbf{y}$ in a row vector for k[th] step in the future:

$$€_k = \frac{[R_{o1} \quad R_{o2} \quad -C_{w1} \quad -C_{w2}]}{(1+\frac{d}{100})^{\frac{k\Delta T}{365}}} \tag{21}$$

It should be noted that even though the costs are represented differently for each layer, they are nevertheless assumed to be the same. Similarly, representing the injection costs (including the discount rate) associated with the inputs $\mathbf{u}$:

$$€_k^{Inj} = \frac{[0 \quad 0 \quad -C_{w,inj1} \quad -C_{w,inj2}]}{(1+\frac{d}{100})^{\frac{k\Delta T}{365}}} \tag{22}$$

The zero values in Eq. (22) correspond to the bottomhole pressures of the input which do not appear in the objective function directly. The NPV objective function in Eq. (18) can be combined with Eq. (21) and Eq. (22) and re-written as follows:

$$NPV = [(€_k \mathbf{y}_k + €_{k+1}\mathbf{y}_{k+1} + ... + €_{k+N}\mathbf{y}_{k+N}) + (€_k^{Inj}\mathbf{u}_k + ... + €_{k+j}^{Inj}\mathbf{u}_{k+N})] \tag{23}$$

Eq. (23), when combined with the parametric model predictions, can be represented by the following matrix form:

$$NPV = \mathbf{f}_1^T \mathbf{u}^N + \mathbf{f}_2^T \tag{24}$$

where, $$\mathbf{u}^N = \begin{bmatrix} \mathbf{u}_k \\ \mathbf{u}_{k+1} \\ . \\ . \\ \mathbf{u}_{k+N} \end{bmatrix} \tag{25}$$

$$\mathbf{f}_1 = \begin{bmatrix} \text{€}_k \mathbf{D} + \text{€}_{k+1}\mathbf{CB} + \text{€}_{k+2}\mathbf{CAB} + ... + \text{€}_{k+N}\mathbf{CA}^{N-1}\mathbf{B} \\ \text{€}_{k+1}\mathbf{D} + \text{€}_{k+2}\mathbf{CB} + ... + \text{€}_{k+N}\mathbf{CA}^{N-2}\mathbf{B} \\ . \\ . \\ \text{€}_{k+N}\mathbf{D} \end{bmatrix} + \begin{bmatrix} \text{€}_k^{Inj} \\ \text{€}_{k+1}^{Inj} \\ . \\ . \\ \text{€}_{k+N}^{Inj} \end{bmatrix} \tag{26}$$

$$\mathbf{f}_2 = \begin{bmatrix} \text{€}_k \mathbf{C}\mathbf{x}_k \\ \text{€}_{k+1}\mathbf{CA}\mathbf{x}_k \\ . \\ . \\ \text{€}_{k+N}\mathbf{CA}^N \mathbf{x}_k \end{bmatrix} \tag{27}$$

The constraints on the inputs $\mathbf{u}$, over the prediction horizon, can be combined in a similar fashion to give:

$$\mathbf{A}_l \mathbf{u}^N \le \mathbf{b}_l \tag{28}$$

Appendix B – Multivariable MPC Formulation

Given the objective function in Eq. (10), minimizing deviation between the output and the set-point over a prediction horizon of P:

$$J = [\sum_{j=1}^{P} (\mathbf{y}_{k+j} - \mathbf{y}_{k+j}^{sp})^T \mathbf{W}_\mathbf{y} (\mathbf{y}_{k+j} - \mathbf{y}_{k+j}^{sp}) + \sum_{j=0}^{M-1} \Delta\mathbf{u}_{k+j}^T \mathbf{W}_{\Delta\mathbf{u}} \Delta\mathbf{u}_{k+j}] \tag{29}$$

Considering the first part of the objective function:

$$J_1 = \sum_{j=1}^{P} (\mathbf{y}_{k+j} - \mathbf{y}_{k+j}^{sp})^T \mathbf{W}_\mathbf{y} (\mathbf{y}_{k+j} - \mathbf{y}_{k+j}^{sp}) \tag{30}$$

$$J_1 = (\mathbf{Y} - \mathbf{Y}^{sp})^T \mathbf{W}_\mathbf{Y} (\mathbf{Y} - \mathbf{Y}^{sp}) \tag{31}$$

where, $$\mathbf{Y}-\mathbf{Y}^{sp}=\begin{bmatrix}(\mathbf{y}_k-\mathbf{y}_k^{sp})\\(\mathbf{y}_{k+1}-\mathbf{y}_{k+1}^{sp})\\.\\.\\(\mathbf{y}_{k+P-1}-\mathbf{y}_{k+P-1}^{sp})\end{bmatrix} \text{ and } \mathbf{W}_\mathbf{Y}=\begin{bmatrix}\mathbf{W}_{y_1}&&&&\\&\mathbf{W}_{y_2}&&&\\&&.&&\\&&&.&\\&&&&\mathbf{W}_{y_P}\end{bmatrix} \tag{32}$$

Using the parametric model in Eq. (4) to predict in the future, it can be shown that

$$\mathbf{Y}=\mathbf{P}_1\mathbf{x}_k+\mathbf{P}_2\mathbf{u}^M \tag{33}$$

where, $$\mathbf{P_1}=\begin{bmatrix}\mathbf{C}\\\mathbf{CA}\\\mathbf{CA}^2\\.\\.\\\mathbf{CA}^{P-1}\end{bmatrix},\ \mathbf{P}_2=\begin{bmatrix}\mathbf{D}&.&.&\mathbf{0}\\\mathbf{CB}&\mathbf{D}&.&\mathbf{0}\\\mathbf{CAB}&\mathbf{CB}&\mathbf{D}&\mathbf{0}\\.&.&.&.\\.&.&.&.\\\mathbf{CA^PB}&\mathbf{CA^{P-1}B}&.&\mathbf{CA^{P-M}B+D}\end{bmatrix},\ \mathbf{u}^M=\begin{bmatrix}\mathbf{u}_k\\\mathbf{u}_{k+1}\\.\\.\\\mathbf{u}_{k+M-1}\end{bmatrix} \tag{34}$$

Combining Eq. (31) and Eq. (33), gives:

$$J_1=(\mathbf{u}^M)^T\mathbf{P}_2^T\mathbf{W}_\mathbf{Y}\mathbf{P}_2(\mathbf{u}^M)+2(\mathbf{u}^M)^T\mathbf{P}_2^T\mathbf{W}_\mathbf{Y}(\mathbf{P}_1\mathbf{x}_k-\mathbf{Y}^{sp}) \tag{35}$$

Similarly, considering the second part of the objective function:

$$J_2=\sum_{j=0}^{M-1}\Delta\mathbf{u}_{k+j}^T\mathbf{W}_{\Delta\mathbf{u}}\Delta\mathbf{u}_{k+j} \tag{36}$$

Working on similar lines as before, Eq. (36) can be re-written as:

$$J_2=(\mathbf{u}^M)^T\mathbf{Q}_2^T\mathbf{W}_{\Delta\mathbf{u}}\mathbf{Q}_2(\mathbf{u}^M)+2(\mathbf{u}^M)^T\mathbf{Q}_2^T\mathbf{W}_{\Delta\mathbf{u}}\mathbf{Q}_1\mathbf{u}_{k-1} \tag{37}$$

where, $$\mathbf{Q}_1=\begin{bmatrix}-1\\0\\0\\.\\.\\0\end{bmatrix}_{M\times1},\ \mathbf{Q}_2=\begin{bmatrix}1&0&.&.&.\\-1&1&0&.&.\\0&-1&1&0&.\\.&.&.&.&.\\.&.&0&-1&1\end{bmatrix},\ \mathbf{W}_{\Delta\mathbf{u}}=\begin{bmatrix}\mathbf{W}_{\Delta u_1}&&&&\\&\mathbf{W}_{\Delta u_2}&&&\\&&.&&\\&&&.&\\&&&&\mathbf{W}_{\Delta u_M}\end{bmatrix} \tag{38}$$

Combining Eq. (35) and Eq. (37):

$$J=(\mathbf{u}^M)^T\{\mathbf{P}_2^T\mathbf{W}_\mathbf{Y}\mathbf{P}_2+\mathbf{Q}_2^T\mathbf{W}_{\Delta\mathbf{u}}\mathbf{Q}_2\}(\mathbf{u}^M)+2(\mathbf{u}^M)^T\{\mathbf{P}_2^T\mathbf{W}_\mathbf{Y}(\mathbf{P}_1\mathbf{x}_k-\mathbf{Y}^{sp})+\mathbf{Q}_2^T\mathbf{W}_{\Delta\mathbf{u}}\mathbf{Q}_1\mathbf{u}_{k-1}\} \tag{39}$$